Interference with the Endosomal Acidification by a Monoclonal Antibody Directed toward the 116 (100)-kD Subunit of the Vacuolar Type Proton Pump

Satoshi B. Sato and Sakuji Toyama*

"Cell and Information," PRESTO, Research Development Corporation of Japan and Department of Biophysics, Faculty of Science, Kyoto University, Kyoto, 606-01, Japan; and *Institute for Virus Research, Kyoto University, Kyoto, 606-01, Japan

Abstract. A monoclonal antibody (OSW2) was prepared by using human osteosarcoma cells. OSW2 was found to be directed toward the 116 (also called 100)-kD protein that uniquely associates to the vacuolar-type proton pump. The antibody specifically localized acidic membrane compartments that could be visualized with acridine orange in many types of human cells. It also reacted with the surface and was internalized along the endosomal pathway. Monitoring the endosome pH by using FITC-dextran and acridine orange suggested that the antibody interfered with low pH. Cell-free experiments indicated that the ATP-dependent acidification was inhibited in endosomes associated with OSW2. In contrast, the antibody gave little effect on the ATPase activity of the solubilized H^+ pump. The internalization of OSW2 reduced infectivity of certain enveloped viruses (influenza, SFV, VSV) by 50 to 80%. Inhibition of viral fusion was directly demonstrated by monitoring the fate of octadecylrhodamine-labeled influenza virus fluorescence. These results indicate that the 116 (100)-kD protein is necessary for the control of pH. The antibody represents a novel probe for understanding the role of the endosomal compartments in cellular physiology.

ENDOCYTOSIS is used by eukaryotic cells to internalize and to process various macromolecular ligands (Goldstein et al., 1985). It also provides an entry pathway for a variety of animal viruses (Marsh and Helenius, 1989). Typically, viruses with a low pH–induced membrane fusion activity, such as members of the orthomyxo-, alpha-, and rhabdo-virus families, uncoat in endosomes (Matlin et al., 1982*a*,*b*; Kielian et al., 1986). During their transfer from the cell periphery to the perinuclear region, they receive increasing acidification and the compartments change morphologically (Gruenberg and Howell, 1989; Dunn and Maxfield, 1992; Mellman et al., 1986). A variety of lysosomotropic reagents alter the processing of internalized ligands and inhibit certain viral infections by equilibrating the pH to that of the culture medium.

Endosomes (Galloway et al., 1983; Yamashiro et al., 1983), as well as coated vesicles (Stone et al., 1983) and lysosomes (Harikumar and Reeves, 1983, Moriyama and Nelson, 1989), have an ATP-driven proton pump that is primarily responsible for acidification. This class of vacuolar (V)[1]-type proton pumps consists of eight to nine different subunits and distributes in many types of acidic compartments in various species (for comprehensive review see Harvey and Nelson, 1992; Forgac, 1989). Recent studies using bovine clathrin-coated vesicles have identified peripheral and integral domains; the former consists of subunits with molecular masses of 73, 58, 40, 34, and 33-kD, while the latter with 116 (or 100)-, 38-, 19-, 17-kD subunits (Adachi et al., 1990). Functionally, the 73 (or 70)- and 58-kD polypeptides are involved in nucleotide binding and hydrolysis (Xie and Stone, 1988; Bowman et al., 1988; Arai et al., 1987; Puopolo et al., 1991; Puopolo et al., 1992), while 40- and 33-kD subunits are in an efficient ATP hydrolytic sector (Xie and Stone, 1988; Hirsch et al., 1988). The smallest subunit, 17 kD, represents the proton channel (Sun et al., 1987; Mandel et al., 1988). The overall architecture is supposed to exhibit a similarity with mitochondrial $F_1F_oH^+$-ATPase by sharing homologous overall structure (Arai et al., 1988; Adachi et al., 1990) and the sequences in certain subunits possess similarities to the ATPase and archaebacteria A-ATPase (Bowman et al., 1988; Manolson et al., 1988; Puopolo et al., 1991; Südhof et al., 1989; Mandel et al., 1988). In contrast, the largest subunit, 116(110)-kD is

Address all correspondence to S. B. Sato, Department of Biophysics, Faculty of Science, Kyoto University, Kyoto, 606-01 Japan. Ph.: (81) 75-753-4216. Fax: (81) 75-791-0271.

1. *Abbreviations used in this paper*: APMSF, (*p*-amidinophenyl)-methanesulfonyl fluoride hydrochloride; CLSM, confocal laser scanning microscopy; DPBS, Dulbecco's PBS; FD, FITC-dextran; HA, hemagglutinin; PFA, paraformaldehyde; p.i., postinfection; R_{18}, octadecylrhodamine; RS, respiratory syncytial; rt, room temperature; TCID, tissue culture infectious dose; TD, TRITC-dextran; Trf, transferrin; V, vacuolar.

unique to the V-type proton pump having minimum homology with known sequences (Perin et al., 1991). Disruption of the gene encoding the corresponding subunit in yeast *Saccharomyces cerevisiae*, *VPH1*, resulted in loss of assembly of the pump in vacuoles (Manolson et al., 1992). The role of this polypeptide in the translocation of proton and in the endosomal pathway in higher eukaryotes is, however, not clear yet.

In the present report, we describe the effect of a mAb that binds cell surface and endosomal compartments. This antibody was found to react with the 116 (100)-kD subunit in the V-type proton pump and internalized along the endosomal pathway. This internalization gave no cytotoxic effect but interfered with the ATP-dependent acidification in endosomes. In support of this effect, the antibody reduced the infectivity of certain types of viruses that uncoat by low pH–triggered fusion. The results suggest involvement of the 116 (100)-kD subunit in the control of endosome functions.

Materials and Methods

Antibodies

A mAb OSW2 (IgG2b) was prepared by a standard hybridoma method using freshly excised human osteosarcoma cells (Hosoi et al., 1982). The antibody was purified from ascites with a protein A–Sepharose column and Fab fragment was prepared by papain digestion according to a standard procedure (Harlow and Lane, 1988). The antibody was labeled either with TRITC (Research Organics, Inc., Cleveland, OH) or biotin-*N*-hydroxysuccinimide ester (Boehringer Mannheim GmbH, Mannheim, Germany) according to the standard procedures (Harlow and Lane, 1989). OST7 is as described (Hosoi et al., 1982). A rabbit antiserum (V759) against a synthetic polypeptide of COOH terminus of the 116-kD subunit of V-proton pump in rat-coated vesicles/synaptic vesicles (Perin et al., 1991) was kindly provided by Dr. T. Südhof (Howard Hughes Medical Institute, Dallas, TX). The following mAbs directed against components of influenza virus A/PR8/34 and Sendai virus were kindly provided by Drs. W. Gerhard and J. Yewdell (The Wistar Institute, Philadelphia, PA): Y8-10C2 (IgG2a), recognizing the acid-induced conformation of the hemagglutinin (HA) (Yewdell et al., 1983), H16L10 (anti-NP), 3C6 (anti-Sendai virus HN). A rabbit anti-influenza serum was the same as described (Bächi et al., 1985). Labeled goat secondary antibodies against mouse and rabbit IgG (FITC, TRITC, or peroxidase) were obtained from Cappel (West Chester, PA) or Nordic Immunology (Tilburg, The Netherlands).

Cells

MRC-5, KB, HEp-2, A549, HT-1080, NRK, 3Y1, Ratec, Rat-2, L, Swiss 3T3, and Vero cells were grown as monolayers at 37°C in Ham F12 (A549) or DME (others) supplemented with 15 or 10% FBS.

Viruses

Egg-grown influenza A virus (A/PR8/34, PR8 virus) and Sendai virus were the same as described (Bächi et al., 1973, 1985). For fluorescence labeling, purified PR8 virus was dialyzed over night at 4°C with 140 mM NaCl (pH 7.2) and reacted for 20 h at 4°C with FITC (Sigma Chem. Co., St. Louis, MO) at 10 μg/2.3 mg viral proteins in 50 mM Na carbonate, 140 mM NaCl (pH 9.5). The mixture was then centrifuged at 100,000 *g* at 4°C for 1.5 h. The pellet was resuspended in Dulbecco's PBS (DPBS) and centrifuged at 2,000 *g* for 5 min. This labeling did not change the hemagglutination titer nor the hemolytic activity at pH 5.5 as measured by using human erythrocyte. A fraction of purified PR8 virus was also labeled with octadecylrhodamine (R_{18}) with a method similar to that described for the labeling of X31 influenza virus (Stegmann et al., 1987). Briefly, to 300 μl (330 μg protein) of virus suspension, 1 μl of 2 mM R_{18} (Molecular Probes, Eugene, OR) in ethanol was rapidly injected. It was incubated for 2 h at (rt) room temperature in the dark. The suspension was passed through a Sephadex G-75 column (0.8 × 15 cm). Labeled virus was obtained in the supernatant after a centrifugation at 7,000 *g* for 5 min. Respiratory syncytial (RS) virus and Polio virus were grown in Vero cells. VSV (Indiana serotype) was passaged in HEp-2 cells. Semliki Forest and Adeno virus type 3 were grown in MRC-5 cells.

Western Blotting

KB or L cells grown at confluency were washed with PBS and scraped. They were solubilized in a sample buffer (63 mM Tris-HCl, 10% glycerol, 2% SDS, 5% 2-mercaptoethanol, pH 6.8) without heating at 100°C. After electrophoresis in 10% polyacrylamide gel (Laemmli, 1970), polypeptides were electroblotted on PVDF membrane (Millipore, Bedford, MA) by using a transfer buffer (50 mM Tris, 380 mM glycine, 20% methanol; Towbin et al., 1979) containing 0.037% SDS. The sheet was then blocked with 5% BSA in TBS (20 mM Tris-HCl, 150 mM NaCl, pH 8.2) and made reacted with antibodies at a dilution of 1:1,000. Bound IgG was detected with gold particles coupled with goat-anti-mouse or rabbit IgGs (Amersham, Intl., Buckinghamshire, UK) in conjunction with silver enhancement. Immunoprecipitate was obtained from KB cells and further analyzed by Western blotting.

Immunofluorescence

In most experiments, coverslip cultures of cells were fixed for 10 min at room temperature with freshly prepared 3% paraformaldehyde (PFA) in PBS. Fixed cells were washed once with DPBS and excess aldehyde was quenched for 5 min at rt with 100 mM glycine in DPBS. Cells were permeabilized for 1 min at rt with 0.5% Triton X-100 in DPBS. They were incubated for 2 h at rt or overnight at 4°C with appropriate dilutions of antibodies. After washing with DPBS, the cells were incubated with secondary antibodies labeled with FITC or TRITC for 1 h at rt. For the detection of surface bound antibodies, live cells were precooled on ice for 10 min, and then incubated for 30 min with antibodies in culture medium (DME) containing 2% FBS. Cells were then washed and fixed overnight at 4°C with 3% PFA-PBS containing 4% sucrose and incubated with secondary antibodies. For double immunofluorescence for the internalized antibody and the residual antigen, cells were incubated firstly with nonlabeled OSW2 in DME-10% FBS at 37°C. After fixation and permeabilization, cells were stained for the antibody with FITC-labeled goat anti-mouse IgG as described above. The residual binding sites of the secondary antibody were blocked by incubation with normal mouse serum for 1 h. The cells were then incubated with biotinylated OSW2 (10 μg/ml in 2% BSA-PBS) for 1 h and it was detected with streptavidin-sulforhodamine 101 (XTRITC-streptavidin; Boehringer GmbH; 10 μg/ml in 2% BSA-PBS) by incubation at rt for 15 min. The specimens were mounted using Mowiol containing 2% 1,4-diazobicyclo [2.2.2] octane (Fluka Chemie, Buchs, Switzerland) and observed in a Reichert Polivar epifluorescence microscope or with a confocal laser scanning microscopy (CLSM) system (MRC-500 or MRC-600, Bio-Rad, Hertsfordshire, UK) mounted on an Axioplan fluorescence microscope (Zeiss, Germany). For comparison of double fluorescence patterns, individual confocal images were merged by the software of the CLSM using green color for FITC, and red for TRITC or XTRITC, respectively.

Estimation of Endosomal Acidity

TRITC-dextran (TD) was synthesized by a reaction for 2 h at rt of aminodextran (40,000 mol wt; Molecular Probes) with TRITC in 50 mM Na Borate (pH 9.0) at an input amine to TRITC ratio of 1:5. The product was purified by a chromatography with a Sephadex G-50 column and by dialysis against DPBS. FITC-dextran (FD 20; Sigma Chem. Co.) was purified as described (Preston et al., 1987). For quantitative fluorescence measurements, the coverslip cultures were incubated for 30 min at 32°C in the presence or the absence of OSW2 (100 μg/ml) with a mixture of FD (5 mg/ml) and TD (250 μg/ml) diluted in EBSS containing 5 mM Na-Hepes, 0.035% $NaHCO_3$, and 0.5% BSA. After a chase of 10 min, cells were mounted for microscopy in EBSS at pH 7.2 or 6.5, with or without 50 mM NH_4Cl and examined within 30 min with the CLSM or a ACAS 570 cytometric system (Meridian Instruments, Okemos, MI). For labeling acidic compartments with acridine orange, cells were washed carefully with DPBS and first incubated for 2 min in the dark with EBSS containing 10 mM Na Hepes, 0.2% BSA, 0.035% $NaHCO_3$, and 20 μM acridine orange (Molecular Probes) as described (Matteoni and Kreis, 1987). In some cases, the observed cells were fixed and permeabilized for indirect immunofluorescence with OSW2 as described above.

Cell-free Assay of Endosome Acidification

Cell-free endosome acidification was assayed after Fuchs et al. (1989).

Briefly, after homogenization of KB cells that had internalized FITC-labeled transferrin in the presence or absence of 100 μg/ml OSW2 for 30 min in TEA buffer (0.25 M sucrose, 10 mM triethanolamine, 10 mM Na acetate, 1 mM Na EDTA, pH 7.2, containing 100 μM (*p*-amidinophenyl)-methanesulfonyl fluoride hydrochloride (APMSF), 10 μg/ml pepstatin A, and 10 μg/ml leupeptin), enriched endosome fraction was obtained at 1 M/0.86 M sucrose interphase. The fraction was treated with 100 μM $NaVO_4$ and incubated in KCl buffer (150 mM KCl, 10 mM tetramethylamine Hepes, pH 7.4, 5 mM $MgSO_4$) at 37°C. Low pH–dependent quenching of FITC fluorescence was initiated by adding an aliquot of ATP stock to a final concentration of 2.5 mM. Fluorescence was measured in a Hitachi 850 fluorescence spectrophotometer.

Preparation of Enriched H^+-ATPase Fraction from Solubilized Endosomes

H^+-ATPase was isolated from the enriched endosomal fraction by using a HiLoad Chromatography System (Pharmacia-LKB, Uppsala, Sweden) after the manner applied for the isolation from plant tonoplast (Parry et al., 1989). The enriched endosome fraction obtained in a similar manner as described above from KB cells on 15 × 500 cm^2 plastic trays (Sumitomo Bakelite, Tokyo, Japan) was pelleted by centrifugation at 150,000 *g* at 4°C for 90 min. The membrane was solubilized in a solubilization buffer (1.2 M glycerol, 4% Triton X-100, 1 mM EDTA, 4 mM $MgSO_4$, 5 mM dithiothreitol, 5 mM Tris-Mes, pH 8.0, containing 100 μM APMSF, 10 μg/ml pepstatin A, and 10 μg/ml leupeptin) by gentle stirring at 0°C for 30 min. After centrifugation at 150,000 *g* for 90 min, the supernatant was applied at 6 ml/h to Sephacryl S300HR (60 × 16) equilibrated with buffer A (10% [vol/vol] glycerol, 0.3% Triton X-100, 0.05 mg/ml type IV-S phosphatidylcholine (Sigma Chem. Co.), 5 mM dithiothreitol, 5 mM Tris-Mes, pH 8.0). The fractions at void volume exhibiting most of the ATPase activity were diluted with 1 vol of buffer B (0.1% polyoxyethylene (10-tridecyl ether ($C_{12}E_8$), 20% (vol/vol) glycerol, 5 mM Tris-HCl, 1 mM EDTA, 4 mM $MgSO_4$, 2 mM dithiothreitol, 0.05 mg/ml type IV-S phosphatidylcholine, pH 6.0) and applied through a Superloop to a Q-Sepharose HR column (16 × 10) equilibrated with the same buffer. The protein was eluted by increasing ionic strength with KCl in buffer B as described (Parry et al., 1989). ATPase activity was eluted in 2 ml exclusively at slightly above 0.2 M KCl, which was identical to the case with the tonoplast. ATPase activity was assayed in the presence of antibodies as in the literature (Parry et al., 1989). The polypeptides were analyzed by 5–20% SDS-PAGE and detected by silver staining (Silver stain kit; Wako Pure Chemicals, Osaka, Japan).

Co-localization of FITC-labeled Influenza Virus and TRITC-OSW2

FITC-labeled influenza PR8 virus (10 μg/ml) and TRITC-OSW2 (300 μg/ml) was co-incubated for 15 min at 37°C with MRC-5 cells. Cells were then treated for 5 min at 37°C with neuraminidase (Sigma Chem. Co.; type V, 10 mU in 50 μl EBSS-BSA). In some cases, cells were pre-cooled at 0°C for 15 min before incubation for 20 min at 0°C with FITC virus and TRITC-OSW2. Cells were then washed with DPBS either at rt or 0°C, and then mounted for microscopy with EBSS-BSA for immediate observation at the dual channel mode of the CLSM.

Monitoring Fluorescence from R_{18}-labeled Virus in Cells

A549 or MRC-5 cells grown on coverslips were incubated for 5 min at 37°C with 50 μl (3 μg/ml) of R_{18}-labeled PR8 virus in DME containing 1% BSA with or without OSW2. Cells were then washed and fixed for 5 min at rt with 3% PFA-PBS containing 4% sucrose, or further chased in the same medium without virus. As a positive control for the inhibition of viral uncoating, cells were preincubated for 15 min at 37°C with 20 mM methylamine or 50 mM NH_4Cl in the medium and then incubated with the same medium containing R_{18}-PR8.

Immunoelectron Microscopy

MRC-5 and HEp-2 cells were fixed for 20 min at rt with 3% PFA and 0.3% glutaraldehyde in PBS containing 4% sucrose, scraped, and further fixed overnight at 4°C in the same solution. The cells were dehydrated with ethanol and embedded in Lowicryl K4M (Carlemalm et al., 1982). Ultrathin sections mounted on formvar-coated gold grids were incubated for 18 h at 4°C with diluted OSW2 ascites fluid (1:500) in 3% BSA-PBS containing 0.1% Triton X-100. After jet washing with PBS, the grids were incubated for 3 h at rt with rabbit anti–mouse IgG Fe. The grids were jet washed again and incubated for 18 h with goat anti–rabbit IgG coupled to colloidal gold (15 nm; Janssen) in 1% BSA-PBS. After jet wash with PBS, the specimen was sequentially treated for 10 sec with PBS containing 0.1% glutaraldehyde and with H_2O. The sections were finally stained with uranyl acetate and lead citrate.

Assays of Virus Infections

Cells grown in 24-well plates or in petri dishes were incubated for 1 h at 37°C in the presence or absence of OSW2 with virus. The cells were then washed with EBSS and incubated for up to 5 d at 37°C in DME containing 2% FBS. Infections were detected by one of the following methods: cytohemadsorption with chicken erythrocytes at 0°C in DPBS, immunofluorescence detection of cytopathic effect, plaque assay or ELISA. For ELISA, the cells in a 96-well plate were fixed for 30 min at rt with 3% PFA and 0.5% glutaraldehyde and the viral antigens were detected with an anti-PR8 rabbit serum by the peroxidase-anti peroxidase method using tetramethylbenzidine as a substrate.

Results

Characterization of OSW2 Antigen

Among mAbs directed against human osteosarcoma cells, OSW2 bound to a polypeptide band with a molecular mass at slightly below 116 kD on the Western blot of KB cell lysates (Fig. 1, lanes *b* and *c*). In contrast, very weak reaction was detected in the L-cell lysate (not shown). The intensity of the polypeptide band was greatly reduced on the blot when cells were solubilized by heating at 100°C regardless of the subsequent treatment with 5 M urea. When SDS was omitted from the electroblotting solution, the transfer of the polypeptides was greatly reduced. These results prompted us to test the possibility whether the polypeptide was the 116 (100)-kD subunit of vacuolar (V-type) proton pump (Stone et al., 1989). Rabbit antiserum against the sequence in the COOH-terminal region of the 116 (100)-kD subunit in rat brain V-type proton pump (V759) displayed a band which coincided with that of OSW2 antigen (Fig. 1, lane *d*). To confirm further the identity between OSW2 antigen and the 116-kD subunit, KB cells lysate was immunoprecipitated with OSW2 antibody and the precipitate was analyzed on a Western blot. The antiserum V759 displayed bands at corresponding position on the blot (Fig. 1, lane *e*). Our preliminary results indicated that antisera raised against a 20–amino acid sequence near the NH_2 terminus (Phe^{37}-Arg^{56}) also detected the polypeptide at 116 kD (result not shown). These results indicate that OSW2 is directed toward the 116-kD subunit of V-type proton pump. Besides the 116 kD and the cross-reaction of secondary anti–rabbit IgG to mouse IgG, V759 detected a smaller polypeptide at around 70 kD (Fig. 1, lane *e*). The intensity of the band varied among experiments. Particularly, the intensity increased when frozen-stored SDS–solubilized sample was analyzed. This likely reflects high lability of the subunit to proteolysis which has been reported in previous studies (Forgac, 1989; Stone et al., 1989; Kane et al., 1992).

Localization of OSW2 Antigen

Immunofluorescence with OSW2 localized vesicular clusters of various sizes around nucleus and minute dots in the peripheral cytoplasm in MRC-5 cells (Fig. 2 *b*). Similar results were obtained in other human cells (KB, A549, HT-1080, and HEp-2). The immunofluorescence pattern was similar to that

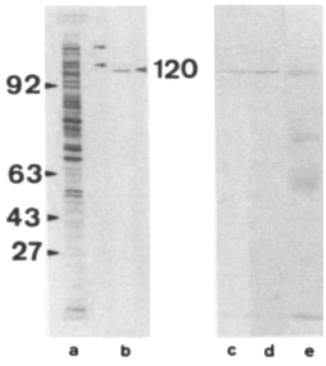

Figure 1. Western blot of OSW2-antigen. Whole KB cell lysate (*a–d*), and OSW2-immunoprecipitate from KB cells (*e*) were Western blotted on PVDF membrane after electrophoresis in 10% gel. They were analyzed for whole proteins with AuroDye forte (*a*), for the antigen of OSW2 (*b* and *c*) and with antiserum against the COOH-terminal sequence of the rat coated vesicles/synaptic vesicles 116-kD subunit (*d* and *e*), respectively. Bound antibodies were detected with goat secondary antibodies conjugated with 10 nm gold, in conjunction with silver enhancement. The small arrows in lane b indicate positions of minor bands. OSW2 and the antiserum localized bands at the identical position (*c* and *d*). The antiserum detected the identical band in the OSW2-immunoprecipitate (*e*), indicating the antigen of OSW2 is the 116-kD subunit of V-type proton pump. The fuzzy band at ca. 50 kD was found to be cross-reaction of gold-anti-rabbit IgG to mouse IgG in the blot.

of acidic compartments which are detectable in living cells with 20 μM acridine orange (Fig. 2 *A*). In contrast, fluorescence in rat cells (NRK, 3Y1, Rat-2, Ratec, and R22) and mouse cells (primary fibroblasts, peritoneal macrophages, and L cells) was not evident (not shown). The distribution of the antigen for OSW2 was also examined by immunoelectron microscopy on thin sections of Lowicryl-embedded MRC-5 and HEp-2 cells. Immunogold reactions resulted in an association with lysosome-like multivesicular structures (Fig. 3). Interestingly, antibody OSW2 was also detectable on the surface of cells incubated at 0°C, where it amounted to 8% of that on fixed-permeabilized culture as determined by using HRP-secondary antibody.

Internalization of OSW2

Since OSW2 bound to the cell surface, we asked whether the antibody was internalized into endosomes. The internalization of OSW2 was mainly examined in MRC-5 cells by immunofluorescence. Specific binding to the surface could be readily detected after incubation for 30 min at 4°C of living cells with OSW2 (50 μg/ml) (Fig. 4 *a*). After a pulse of 5 min followed by chase in antibody-free medium at 37°C, the antibody was detected in small peripheral vesicles (Fig. 4 *b*). Between 30–60 min, an increasing number of fluorescent spots distributed over the whole cytoplasm (Fig. 4 *c*). After 3 h, some of them had an increased size and accumulated in the perinuclear region (Fig. 4 *d*). Internalization of Fab fragment of OSW2 resulted in a similar pattern of fluorescence during the first hour, whereas at later time-points, the fluorescence became weaker, suggesting proteolytic degradation (data not shown). Other human cells (HEp-2, A549, and HT-1080) internalized OSW2 in a similar fashion, whereas rat cells never produced a detectable fluorescence with OSW2, nor did mouse antibody from nonimmune serum (100 μg/ml) in MRC-5 cells under this condition.

In contrast to the vesicular patterns of the antibody detected in fixed and permeabilized cells, the compartments localized in living cells by an incubation for 15 min at 37°C with 300 μg/ml TRITC-OSW2 represented a mixture of vesicles and tubules (Fig. 4 *e*). The tubular pattern was also seen in cells after an incubation under the same condition with a fluid phase marker TRITC-dextran (5 mg/ml) (Fig. 4 *f*). The tubules were not seen when cells were fixed with 3% PFA-PBS.

To trace the internalization pathway of OSW2, cells continuously incubated with an excess amount of nonlabeled OSW2 (100 μg/ml) at 37°C were examined by double immunofluorescence using the biotinylated antibody (Fig. 5). While biotinylated OSW2 in conjunction with XTRITC-streptavidin localized the antigen in nontreated cells similarly to conventional immunofluorescence (Fig. 5*a*, compare to Fig. 2 *B*), its fluorescence gradually decreased by endocytic internalization of the nonlabeled antibody. At 30 min, FITC-immunofluorescence for the internalized OSW2 localized compartments distributing in the cellular extensions and

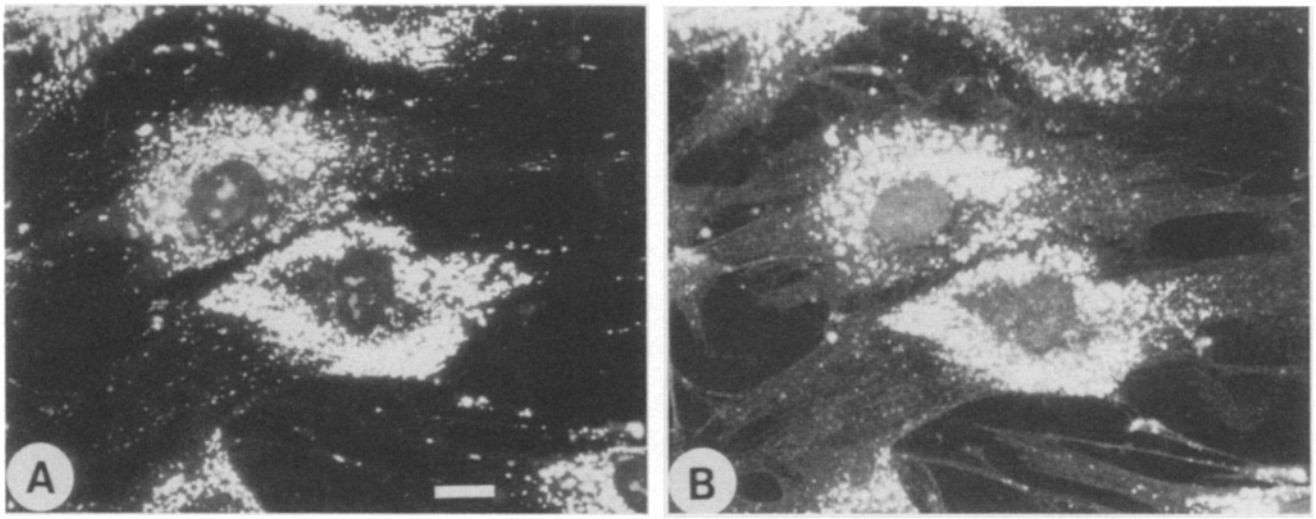

Figure 2. Localization of OSW2 antigen in MRC-5 cells. Conventional fluorescence microscopy of living cells after staining of acidic vesicles with acridine orange (*A*) followed by fixation and indirect immunofluorescence of the same cell with OSW2 (*B*) reveals an identical pattern of distribution of the two fluorescences. Bar, 20 μm.

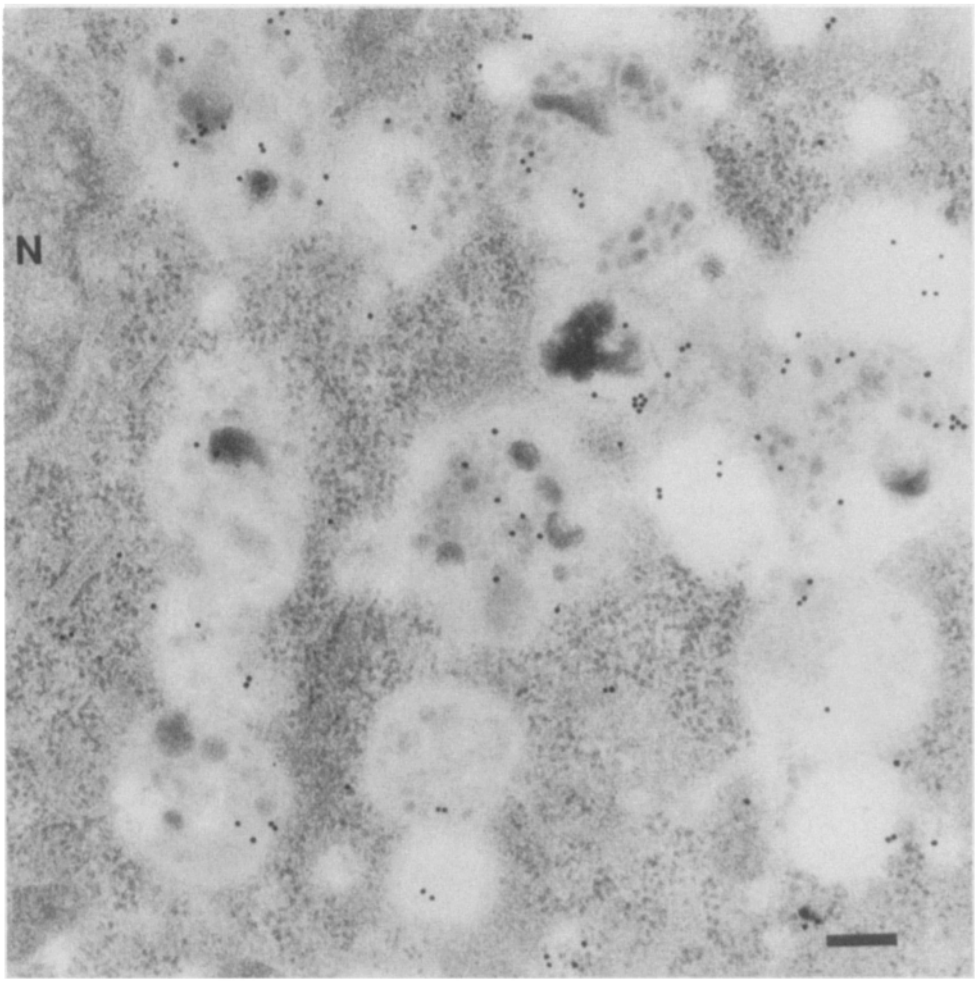

Figure 3. Immunoelectron microscopic localization of OSW2 antigen in HEp-2 cells. Ultrathin sections were reacted with OSW2 followed by rabbit anti-mouse IgG Fc and goat anti-rabbit IgG-gold particles (15 nm) which are predominantly reacting with multivesicular structures near the nucleus (*N*). Bar, 200 nm.

one side near the nucleus without XTRITC-immunofluorescence (Fig. 5 *b*). The residual antigen was localized in a cluster at one side of the nucleus and in peripheral region. In 1 h, more FITC-fluorescence localized perinuclear compartments which also exhibited XTRITC-fluorescence, giving yellowish color in the merged image (Fig. 5 *c*). On the other side of the nucleus, the compartments remained associated purely by XTRITC-immunofluorescence but they decreased in number. In 3 h, the compartments with FITC-fluorescence further increased in number, while XTRITC-immunofluorescence was greatly reduced (Fig. 5 *d*). The compartments with both the fluorescences, giving yellowish color also became very few. The double immunofluorescence pattern did not change further by the prolonged incubation (not illustrated). These results indicate that internalized OSW2 progressively distributed in most of the endocytic compartments that are associated with the antigen. However, the results also indicate the presence of the compartments that persistently free from the binding of the internalized OSW2. These results suggest either that the antibody is degraded before reaching there or that, on entering into lysosomes, the antibody is degraded and/or turns into a nonfixable dissociated form.

No cytopathic effect was detected by observation with phase contrast optics after the incubation of cells with OSW2 under the pulse–chase condition or a continuous incubation for 3 d at 100 μg/ml OSW2. The growth curve of KB cells was identical to that in the absence of the antibody (not shown).

OSW2 Interfered with Endosomal Acidification

The effect of the internalization of OSW2 on the endosomal pH was examined in a confocal microscope using a combination of FD and TD (Fig. 6). In contrast to the quenched fluorescence of FD (5 mg/ml) in cells without OSW2 (Fig. 5 *c*), the intensity of fluorescence in some tubular compartments was significantly higher in the presence of the antibody (Fig. 6 *a*). The endocytic activity as measured with horse radish peroxidase was the same as the control culture at this temperature (not shown). The intensity of TRITC-fluorescence was also very similar. These results rule out the possible dependence of the fluorescence intensity per unit amount on the concentration of fluorophore (see Wells et al., 1990). Although a very high detection sensitivity which has been demonstrated to be necessary for accurate determination of small targets (Zen et al., 1992) was not attained in the present research, the ratio of FD-fluorescence to that of TD in whole cells was readily analyzed by a 16-bit (4,096) gray scale of the Acas cytometric system. It was also noted that 50 mM NH_4Cl used for equilibration of pH induced a vesiculation of the tubular endosomes into small and moving

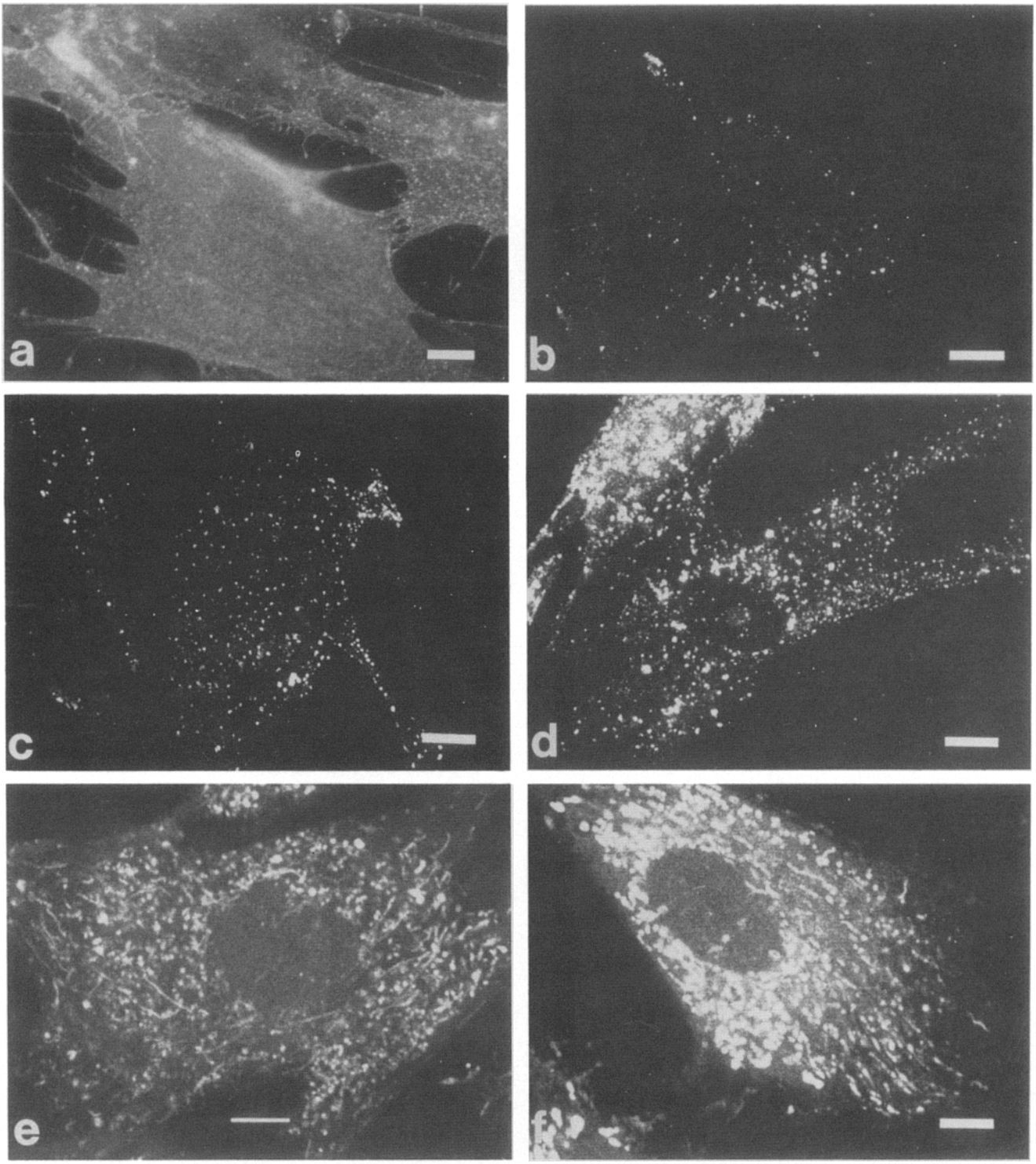

Figure 4. Binding of OSW2 (50 μg/ml) to the surface of MRC-5 cells is detectable by indirect immunofluorescence after an incubation for 30 min at 4°C followed by fixation and subsequent reaction with anti-mouse IgG-TRITC (*a*). Endocytosis of OSW2 is shown by CLSM after an incubation for 5 min at 37°C and a chase in antibody-free medium for 5 min (*b*), 25 min (*c*), and 3 h (*d*). Internalized mAb was detected after fixing and permeabilizing the cells by a reaction with anti-mouse IgG-TRITC. When TRITC-OSW2 (300 μg/ml) was added at 37°C for 15 min and the cells were observed without fixation, the antibody was internalized in tubular compartments (*e*). Cells incubated with TD (5 mg/ml) under the same condition also showed tubular compartments (*f*). Bars, 10 μm.

structures (see Fig. 10), thereby making fine estimation of fluorescence in each structure difficult. The integrated FD normalized by TD-fluorescences in the presence of OSW2 amounted to 62% of that measured in cells incubated at pH 6.5 in the presence of 50 mM NH_4Cl, while that in the absence of OSW2 amounted to 29%. The estimated pH was 5.2 for control, while in the presence of OSW2, it was 5.8.

In contrast to the effect on the earlier compartments, acri-

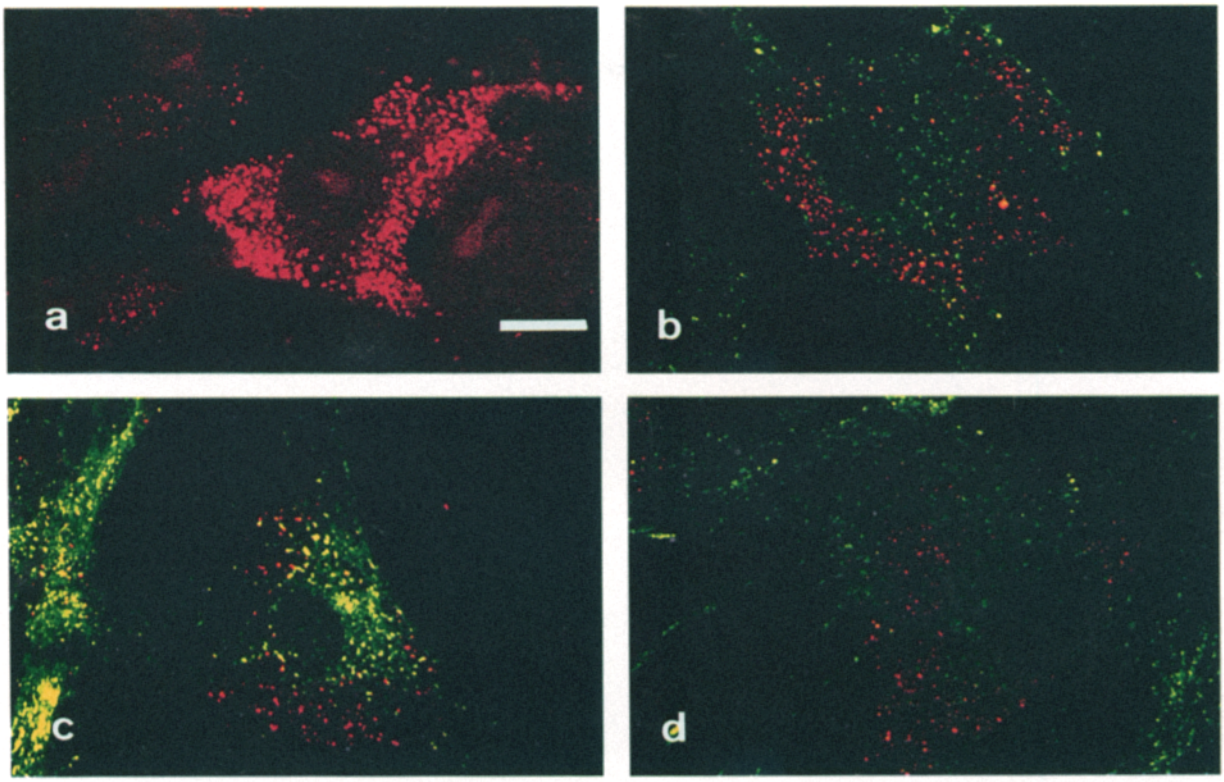

Figure 5. Internalization of OSW2 by its continuous presence during incubation and the distribution of the residual antigen as detected by biotinylated OSW2 after fixation. Cells were incubated for 0 (*a*), 30 min (*b*), 1 h (*c*), and 3 h (*d*), respectively, with nonlabeled OSW2 (100 μg/ml) at 37°C. After fixation, the antibody was localized by FITC-anti-mouse IgG (*green*). Residual antigen was detected by biotinylated OSW2 in conjunction with XTRITC-streptavidin (*red*) after blocking the binding sites of FITC-antibody by a mouse serum. Internalized OSW2 gradually distributed in the endosomal compartments with concomitant reduction of the free antigen. In 1 h, compartments with both the substantial immunofluorescence can be depicted by yellowish color which typically clustered near the nucleus (*c*). In 3 h, XTRITC-immunofluorescence was restricted to the compartments in a limited region (*d*). Bar, 20 μm.

dine orange detected a cluster of acidic vesicular compartments in the perinuclear region even after an incubation for 3 h with the antibody (50 μg/ml) at 37°C (Fig. 6 *e*). Weaker fluorescence was observed in some compartments but the major parts were similarly fluorescent. These results suggest that OSW2 gives more limited effect on the lysosomal pH. Complete abolition of staining was only achieved by equilibration of the vesicular pH with that of the medium (pH 7.2) by agents such as 50 mM NH_4Cl. These results made contrast to the action of a specific inhibitor of V-type proton pump, bafilomycin A_1 (Yoshimori et al., 1991), where the average pH was elevated to a similar degree.

OSW2 Interfered with ATP-dependent Acidification of Endosomes in a Cell-free System but not with the ATPase Activity

To address the effect of internalized OSW2 on proton translocation more directly, acidification of endosomal lumen was assayed in a cell-free system (Fig. 7). Enriched endosomal fraction isolated from KB cells that had been incubated with FITC-transferrin (Trf) rapidly quenched its fluorescence upon incubation with 2.5 mM ATP. The degree and kinetics were in good agreement with the literature (Fuchs et al., 1989). The acidification was not influenced by the pretreatment with 100 μM $NaVO_4$. It was, however, inhibited by the presence of 100 μM $ZnCl_2$, which has an inhibitory effect on the Cl^- channel (see Hille, 1992) (results not shown). When cells were coincubated with 100 μg/ml OSW2, the FITC-fluorescence and the density of the endosomes after the homogenization were virtually the same. However, internalization of OSW2 inhibited the generation of low pH, indicating that the luminal association of OSW2 inhibited ATP-dependent acidification.

Zhang et al. (1992) have shown that the sole presence of the integral domain of the proton pump in coated vesicle or in reconstituted lipid vesicles does not show specific proton conductance. We tested if binding of OSW2 turned off the proton movement. For this purpose, the enriched endosomal fraction was preincubated with 50 mM NH_4Cl at 0°C and the pH inside was lowered by dilution. This procedure decreases pH which is released by NH_4^+ to penetrate through the membrane in the neutral form NH_3. When the endosomes were diluted in 10 vol of KCl buffer, FITC-fluorescence was rapidly quenched. The fluorescence slowly returned to the original level in 15 min through the redistribution of proton. When endosomes that had internalized OSW2 were treated, the recovery, particularly the early phase, was rather accelerated with a factor of 1.5 (Fig. 7 *b*).

To test the possibility that the binding of OSW2 directly inhibits the ATPase activity, we isolated the pump assembly from the enriched endosomal fraction by a combination of gel-filtration and ion-exchange chromatography. In Q-Seph-

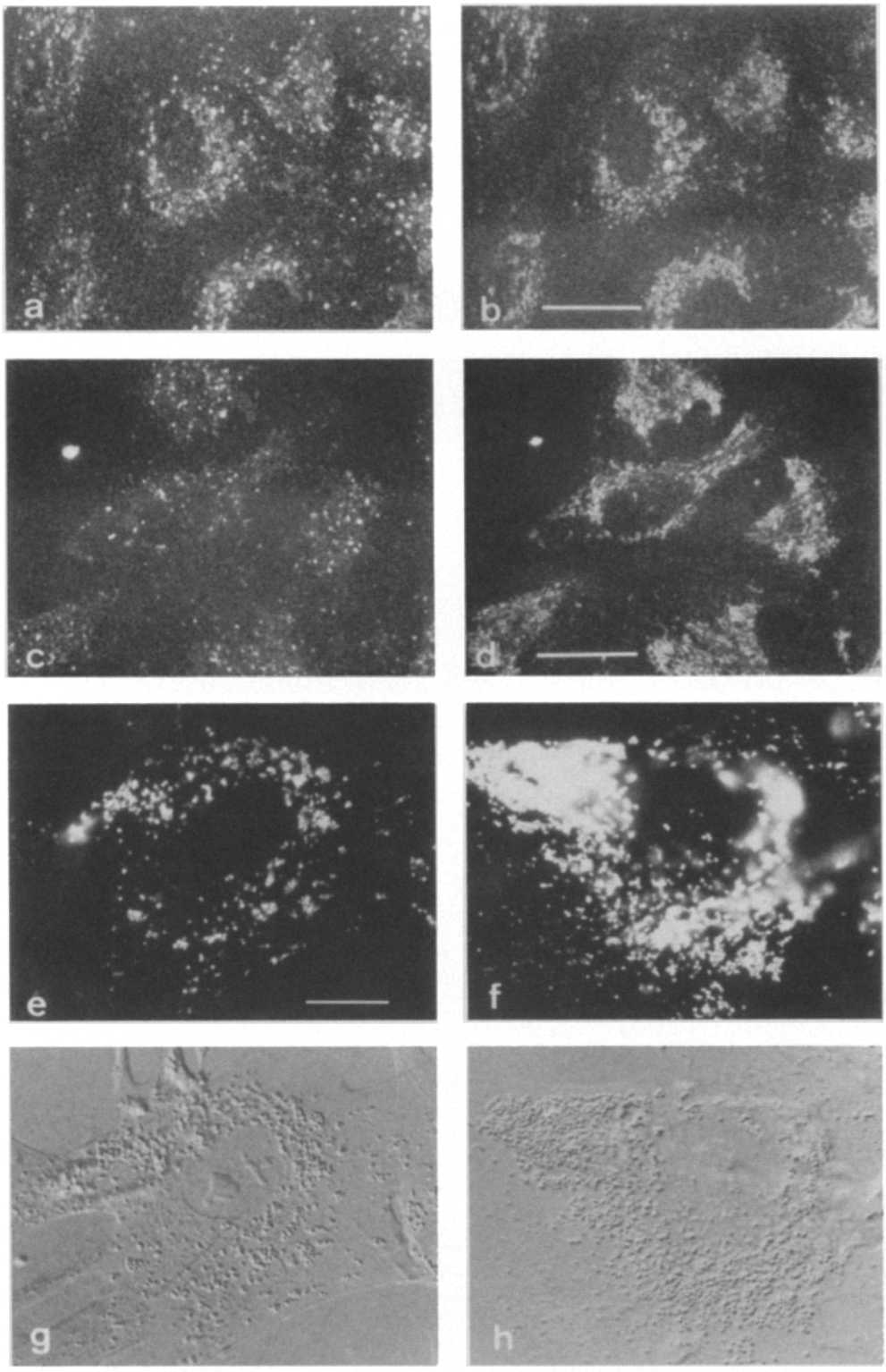

Figure 6. Effect of OSW2 on endosomal acidification after an incubation for 30 min at 32°C of A549 cells with FD (5 mg/ml) and TD (0.25 mg/ml) in the presence (*a* and *b*) and absence (*c* and *d*) of OSW2 (100 μg/ml). FITC fluorescence (*a* and *c*) in endosomes localized by co-internalized TD (*b* and *d*) was stronger in the presence of OSW2. However, OSW2 did not abolish the staining with acridine orange in MRC-5 cells even 3 h after the internalization (compare *e* to *f*). *g* and *h* show corresponding DIC images. Bars: (*b* and *d*) 10 μm; (*e*) 20 μm.

arose column, the ATPase activity of enriched endosome fraction from KB cells was eluted exclusively at the same salt concentration as in the isolation of plant tonoplast V-ATPase (Parry et al., 1989) (result not shown). The specific activity was 3.7–7.0 μmol/mg/min. The pattern of SDS-PAGE showed the typical V-type proton pump although some contaminating bands were visible (Fig. 8 *a*). Among these, one at slightly above 70 kD increased upon storage at 0°C with concomitant decrease of the 116-kD subunit, suggesting proteolytic degradation. The ATPase and OSW2 (20–100 μg) were preincubated at room temperature for 30 min and the reaction was initiated by adding ATP to 3 mM. The presence of the antibody reduced the activity only by up to 13% (Fig. 8 *b*), which is at the similar level as a control unrelated antibody. These results indicate that binding of OSW2 to the 116 (100)-kD subunit in the pump does not interfere with the

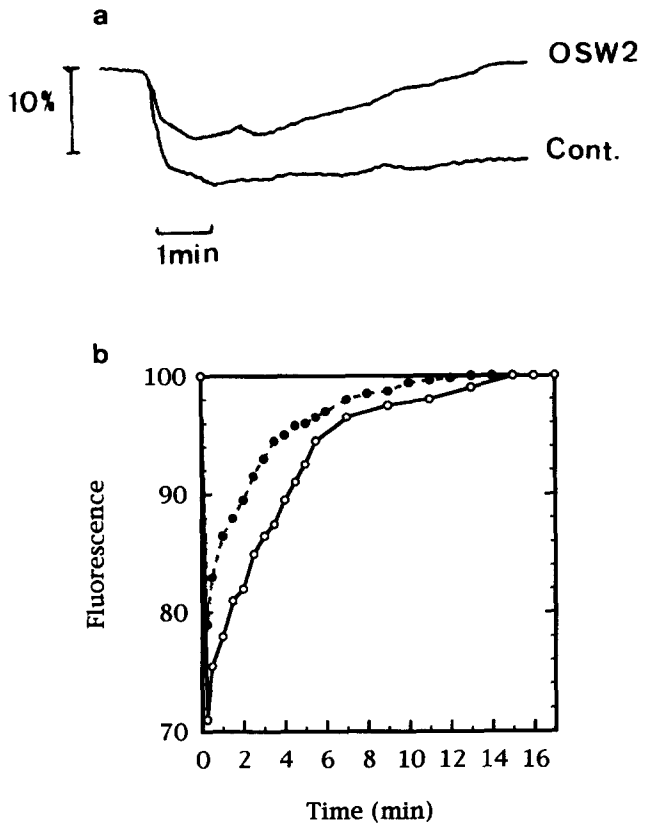

Figure 7. (*a*) OSW2 interfered with ATP-dependent acidification of endosomes in vitro. Enriched endosome fraction was prepared from KB cells incubated with FITC-Trf in the presence and the absence of 100 μg/ml OSW2. The fluorescence of control vesicles was quenched by addition of ATP, while the quenching was reduced in the presence of the antibody. (*b*) The endosome fractions were equilibrated with 50 mM NH_4Cl for 10 min and injected in 10 vol of NH_4Cl-free KCl-buffer. In the absence of OSW2 (○), fluorescence was rapidly quenched by release of proton from NH_4^+ and slowly returned to the original level. In contrast, the recovery was slightly accelerated by the presence of OSW2.

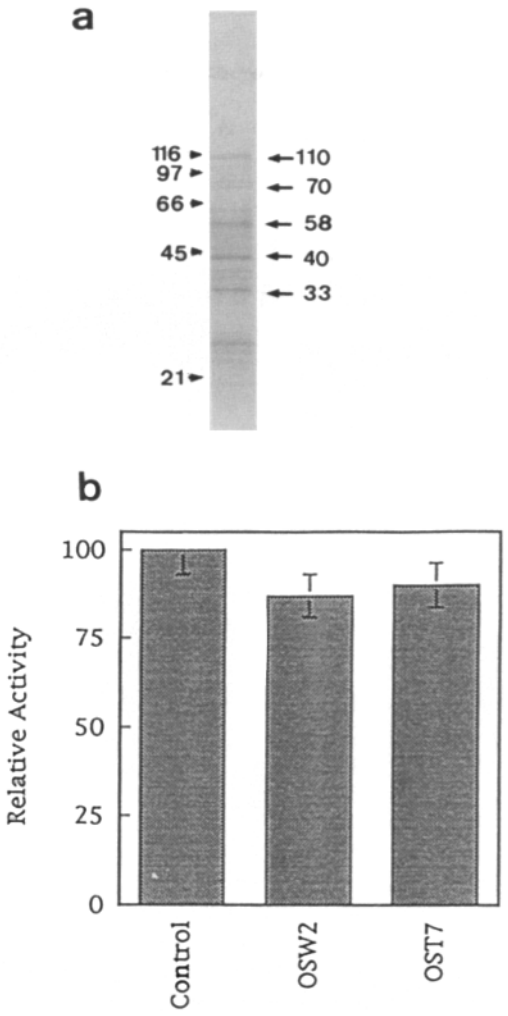

Figure 8. (*a*) A SDS-PAGE pattern of H^+-ATPase isolated from enriched endosome fraction. The polypeptides were detected by silver staining. Arrow heads indicate the positions of molecular weight standards. Values with arrows indicate estimated molecular masses of some bands. (*b*) The ATPase fraction was incubated with OSW2 or OST7 (a mAb directed toward the alkaline phosphatase) for 30 min, then assayed for ATPase activity. The antibodies gave little effect on the activity.

ATP hydrolysis. The antibody precipitated the 116 (100)-kD subunit from the isolated pump, while the recovery of other subunits varied among experiments (result not shown). Whether the antibody-binding dissociated other subunits or they were simply lost during the wash of the immunoprecipitate was not clear.

Effect of OSW2 on Influenza Virus Infection

There is considerable evidence that low pH of the endocytic compartments triggers fusion of certain viruses with host cell membranes (Marsh and Helenius, 1989). We asked if OSW2's interference with the acidic environments in endosomes could inhibit the infection of influenza virus. The effect of internalization of antibody OSW2 on the infection of influenza virus PR8 (1 HAU/0.12 μg protein) was examined by incubating for 1 h at 37°C with 1–2 × 10^4 MRC-5 cells. The cells were then washed and incubated in fresh medium containing 2% FBS. By ELISA, OSW2 IgG (10 μg/ml) inhibited by 50–80% at 18 h postinfection (p.i.) (Fig. 9). Though to a reduced extent, Fab fragment of OSW2 (10 μg/ml) was also inhibitory. The inhibition was also seen as assessed by cytohemadsorption at 18 h or immunofluorescence using anti NP antibody at 4 h. By end-point titration of cytohemadsorption, coincubation of cells with virus and antibody OSW2 and addition of antibody alone for 1 h prior to the infection of cells with the virus resulted in the same degree of inhibition. When antibody was previously made bound to the cell surface at 0°C, the inhibition was still seen but reduced by a factor of 2. In contrast, when added 1 h after the inoculation, OSW2 failed to inhibit the infection. No reduction of the infection was observed in rat or mouse cells to which binding of the antibody was not significant. These results suggest that reduction of the infectivity is mediated by interference with the early step of the entry pathway through specific antibody binding to endosomes.

OSW2 (100 μg/ml) did not influence the hemagglutination titer of the virus nor the hemolytic activity at pH 5.5 (not

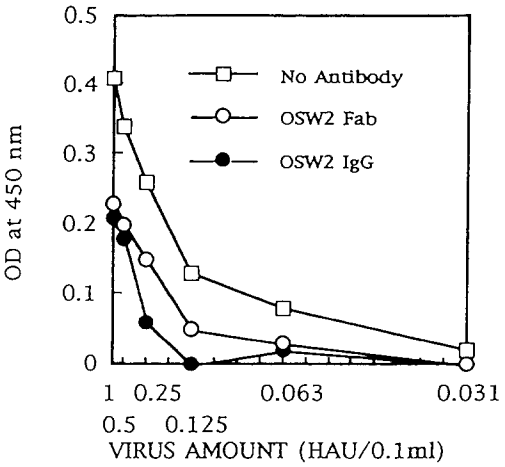

Figure 9. Inhibition of infection by influenza virus PR8 by OSW2 antibody. MRC-5 cells in a 96-well plate (1×10^4 cells/well) were incubated for 1 h at 37°C with OSW2 (10 μg/ml) and with serial dilutions of virus. Cells were fixed 18-h p.i. and virus antigen was determined with an ELISA assay using rabbit anti-PR8 serum in conjunction with peroxidase-anti-peroxidase method.

shown). The amount of fluorescently labeled virus bound on the confluent culture at 0°C after 30 min, and after subsequent incubation at 37°C for 30 min was within experimental errors (1.05 ± 0.08 and 1.02 ± 0.06, compared to the controls, respectively). No evident change in the surface-binding pattern was detected by fluorescence microscopy of cells incubated for 30 min at 4°C (not shown).

Co-internalization of virus particles and OSW2 into cells was monitored by double fluorescence experiments. After incubation for 15 min at 37°C with a mixture of FITC-labeled PR8 and TRITC-OSW2, cells were observed in CLSM without fixation. The punctate FITC-fluorescence contrasted to the tubular pattern of TRITC-fluorescence (Fig. 10, *a* and *b*). Addition of 50 mM NH_4Cl to the incubation medium resulted in a vesiculation of the compartments containing OSW2 (Fig. 10, *c* and *d*). Comparison by merging the two patterns of fluorescence using the software indicated the colocalization of the major part of the virus and the antibody-associated compartments. When the virus and the antibody were adsorbed to the cell surface by a coincubation for 15 min at 0°C and observed in 5 min at 20°C, the fluorescence of virus and antibodies was almost exclusively colocalized (Fig. 10, *e* and *f*).

Fusion of the viral and endosome membranes was studied by labeling virus with a self-quenching concentration of a fluorescent membrane probe octadecylrhodamine (R_{18}). We used confocal imaging of single fixed cells rather than measuring a suspension of living cells in a spectrofluorometer (Stegmann et al., 1987; Nussbauman and Loyter, 1987). This was because the release of bound virus due to the viral neuraminidase during the incubation at 37°C could not be neglected and also because significant delay in the endosome transport was assumed in a suspension culture of normally attached cells. A549 cells were incubated at 37°C with the labeled virus (3 μg/ml) in the presence or absence of OSW2 and fixed at various time points. After 10 min, the fluorescence of cell-associated virus and of free virus (adsorbed to the cover slip) remained unchanged in the presence and absence of OSW2 (not shown). After 30 min, bright and polymorphic fluorescent spots appeared in the cells incubated in the absence of OSW2 (Fig. 11 *a*). The relative intensity of this fluorescence was determined by the image processing software of the CLSM. The dequenched fluorescence of the large spots comprised 20–100% of the 8-bit (256 values) intensity histogram, while the spots with quenched fluorescence (10 min of incubation) had <10% of the maximal value. The presence of OSW2 inhibited the dequenching of the fluorescence (Fig. 11 *b*) to the same degree as did a preincubation for 15 min with 50 mM NH_4Cl (Fig. 11 *d*) or with 20 mM methylamine. The inhibition of dequenching by these amines was less efficient than by OSW2 when cells were not preincubated with them before the addition of R_{18}-labeled virus (Fig. 11 *c*). These results confirmed the failure of fusion in cells internalized OSW2. This could be also demonstrable by the lack of acid-induced conformation of hemagglutinin glycoprotein by using a specific antibody Y8-10C2 (results not shown).

Effect of OSW2 on the Infection of Various Viruses

After characterizing the effect of OSW2 on the infection with influenza virus PR8, a variety of other virus types were studied. Viruses and the antibody (100 μg/ml) were incubated for 1 h at 37°C with cells and the progress of infection was examined (Table I). As further examples of enveloped viruses with an endosome route of entry, VSV and SFV were examined. In plaque assays of VSV-infection in HEp-2 cells, OSW2 reduced the number of plaques to 20% of the controls. SFV infection ($2–10 \times 10^4$ tissue culture infectious dose (TCID) for 10^4 MRC-5 cells) was scored 10-h p.i. by a titration of the infectivity in the culture supernatant on Swiss 3T3 cells. In cultures treated with OSW2, the highest dilution capable to induce a cytopathic effect was reduced by 80%.

As examples of viruses with pH-independent fusion activity, the infection of cells with Sendai virus and RS virus was examined. OSW2 had no detectable inhibitory effect on infections of MRC-5 cells with Sendai virus, as examined by end-point titration of cytohemadsorption (18-h p.i.) and immunofluorescence with anti-HN antibody (12-h p.i.). The extent of infection at various multiplicity of infection was not changed by OSW2. Infections of HEp-2 cells with RS virus were scored microscopically by detection of the formation of syncytia and of cells expressing F protein which was visualized by immunoperoxidase methods. At 18 p.i., the number of infected cells was the same in presence or absence of OSW2.

OSW2 was also tested in conjunction with infections by the nonenveloped viruses Polio and Adeno (type 3). These viruses developed a cytopathic effect in MRC-5 cells within 24-h p.i. regardless of the presence of OSW2. Adenovirus infection examined at 48-h p.i. by plaque assays using A549 cells showed 25% reduction as a result of pre- or coincubation with OSW2. No reduction of the infectivity was observed in the infection of A549 cells by polio virus.

Discussion

A monoclonal antibody OSW2 was found to bind to the largest subunit of the V-type proton pump, 116 (100)-kD (Fig. 1). The subunit uniquely associates to the pump and

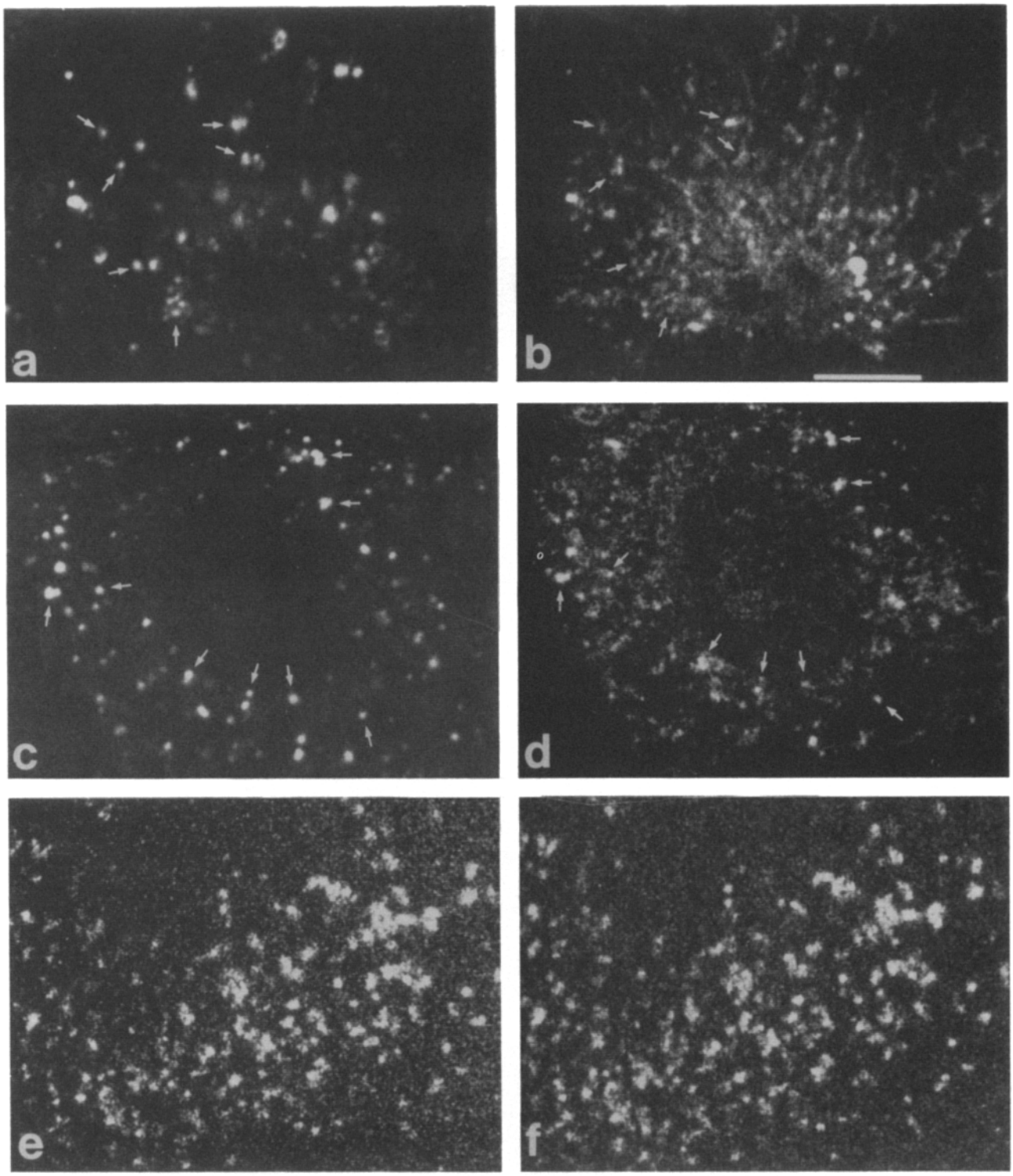

Figure 10. Colocalization of influenza virus and OSW2. Cells were coincubated at 37°C for 15 min with FITC-PR8 virus (10 μg/ml) and TRITC-OSW2 (300 μg/ml) followed by 5-min chase in a fresh medium containing neuraminidase. Many of the virions (*a*) were localized in limited regions of the tubular compartments (*b*). Some particles were localized in places without TRITC-fluorescence. In cells mounted in medium containing 50 mM NH_4Cl, tubular endosomes were fragmented and the virus was largely colocalized with them (*c* and *d*). When the virus and the antibody was added to the cells at 0°C for 20 min and immediately observed at room temperature, the virus and the antibody were almost exclusively colocalized (*e* and *f*). Bar, 10 μm.

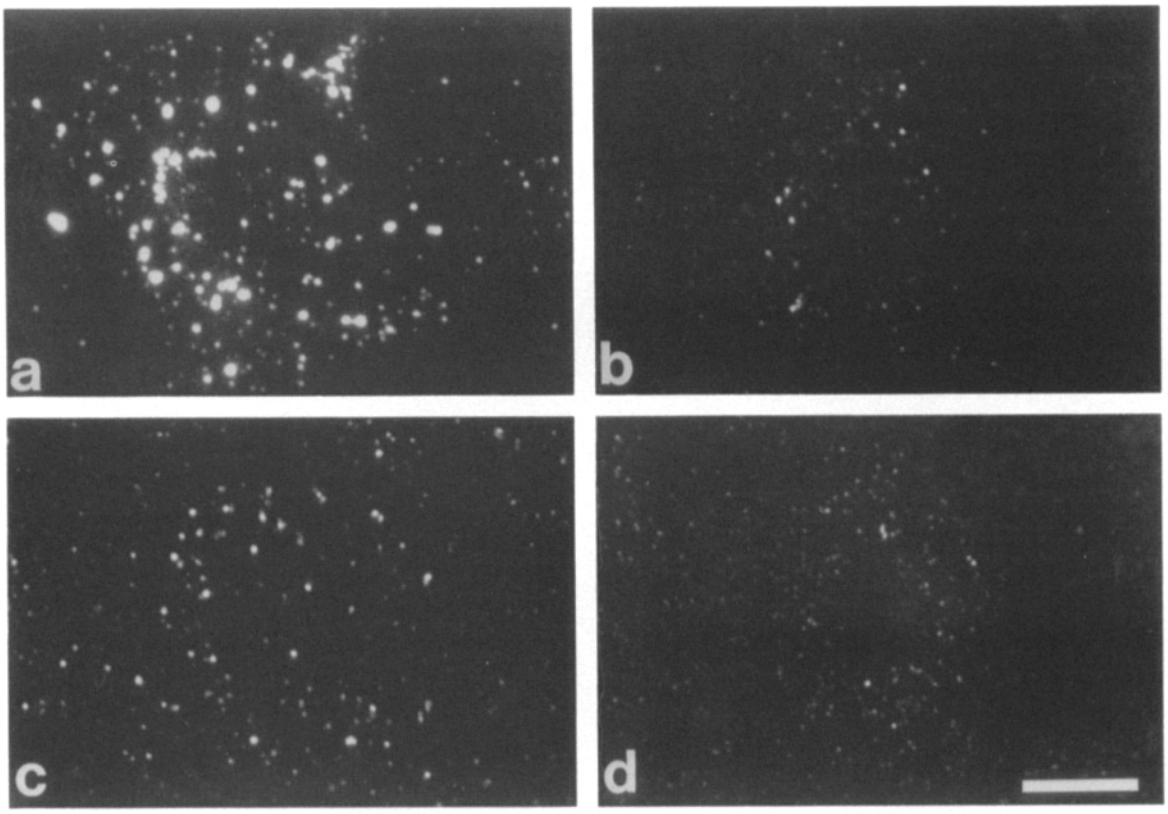

Figure 11. Comparison of the inhibition of dequenching of R_{18}-labeled PR8 virus by OSW2 and by NH_4Cl. Cells were incubated for 10 min at 37°C with the virus (3 μg/ml) and in presence or absence of OSW2 (50 μg/ml) or NH_4Cl (50 mM) followed by chase for 20 min. Viruses in untreated cells reveal extensive dequenching of fluorescence as a result of fusion in the endosomes (*a*), but, in the presence of OSW2, little dequenching is detectable (*b*). In the presence of NH_4Cl, viruses internalized into cells show reduced but significant dequenched fluorescence (*c*), whereas pretreatment of cells with NH_4Cl followed by incubation with virus in the presence of NH_4Cl again resulted in quenched fluorescence (*d*). Bar, 20 μm.

distributes not only in mammalian acidic compartments but also in plants and in yeast with a mass ranging 95 to 100 kD (Parry et al., 1989; Kane et al., 1989). The predicted secondary structure of the 116 (100)-kD from the cDNA sequence in rat clathrin-coated vesicles/synaptic vesicles indicates a bipartite structure with a hydrophilic amino terminus and a carboxyl-terminal region containing eight hydrophobic domains (Perin et al., 1991). Unlike other subunits, the lack of a similar polypeptide in other classes of ATPases (i.e., F_1F_o-ATPase and A-ATPase) and some specific reasons including high susceptibility to proteolysis (Forgac, 1989) and lability to form an aggregate during solubilization for PAGE (Stone et al., 1989) have hampered its biochemical characterization. Although genetic studies of yeast have suggested its role in the assembly of peripheral subunits (Kane et al., 1992; Manolson et al., 1992), the mode of involvement of

Table I. Effect of OSW2 on the Infection of Viruses

Virus	Host cell	Virus per 10^4 cells*	Inhibition by OSW2‡
Influenza (PR8)	MRC-5, A49, HEP-2	0.06-4 HAU	50–80% (ELISA, CHA)§
Influenza (PR8)	Rat-2, R22, Ratec	0.05-2 HAU	0% (CHA)
VSV	MRC-5, HEp-2	(0.5–70) × 10^4 PFU	80% (plaque)
SFV	MRC-5	64–2 × 10^4 TCID	80% (TCID)
Sendai	MRC-5	0.16–2.5 HAU	0% (CHA)
RS	HEp-2	1/(2,500–125) dilution of stock	0% (IPO)‖
Adeno type3	MRC-5, A549	2–6 × 10^4 PFU	<25% (plaque)
Polio	MRC-5, A549	6 × 10^2–10^4 PFU	0% (TCID)

* Infection was monitored by various methods described in Materials and Methods using indicated amount of virus.
‡ Inhibition was calculated by indicated methods as follows: (value without OSW2 − value with OSW2)/(value without OSW2).
§ End-point titration of cytohemadsorption.
‖ Immunoperoxidase.

the subunit in the ATP-dependent proton translocation and the endosome functions were not yet elucidated. In the present study, the effects of OSW2 inhibiting quenching of FITC-fluorescence in endosomes both in vivo (Fig. 6) and in vitro (Fig. 7) indicate that the 116 (100)-kD subunit is indispensable for the endosomal acidic environment.

The V-type pump consists of peripheral (Vi) and integral (Vo) domains (Zhang et al., 1992; Puopolo and Forgac, 1990). The membrane-spanning domain consists of one each copy of 116 (100)-, 38-, 19-, and six copies of 17-kD subunits (Zhang et al., 1992). In yeast, the 95-kD subunit is targeted to the vacuole independently of the peripheral subunits as long as the proton pore, 17-kD, is present (Kane et al., 1992). This targeting to vacuoles appears to be similar to other proteins, which, in contrast to mammalian cells, represents the default pathway (Roberts et al., 1992). When OSW2 was applied to human cells, it bound to the cell surface and was transported along the common endocytic route (Figs. 4 and 5). When Fab fragment of the antibody was applied, it was similarly transported but readily lost its antigenicity at the time point of lysosomal delivery. The binding did not interfere with the internalization of fluid markers, nor of influenza virus. These results strongly suggest that binding of OSW2 does not interfere with the endocytic trafficking of the subunit from the cell surface nor the movement of the membrane compartments. Inhibition of the acidification in OSW2-associated endosomes in a cell-free system (Fig. 7 *a*) strongly suggests that the antibody-binding interferes with the function of the 116 (100) kD in endosomes but not the association of the 116 (100)-kD subunit in the compartments per se.

In yeast, the corresponding subunit of the 116 (100) kD has been shown to be in close contact with some peripherally associating catalytic subunits since epitope sites of the former are blocked by the latter (Kane et al., 1992). This interaction appears to be crucial for the assembly of peripheral subunits since disruption of the gene encoding the largest subunit mislocalizes ATP-binding subunits (69 and 60 kD) (Manolson et al., 1992). Taking the homology of the architecture to that of mitochondrial F_1Fo-ATPase, these results also suggest involvement of the interaction in coupling of ATP hydrolytic energy to proton translocation. It is likely that binding of OSW2 to the 116 (100)-kD subunit either interfered with the association of other subunit(s) or uncoupled the catalytic reaction to the translocation of proton. Because OSW2 did not inhibit ATPase activity of the solubilized pump, the 116 (100)-kD subunit is unlikely to be directly involved in the hydrolysis by the already assembled one.

Studies on the pump isolated from coated vesicles have indicated that neither the sole presence of the integral domain reconstituted in lipid vesicles nor the one lacking the peripheral domain in the original vesicles show specific proton conductance (Zhang et al., 1992). In contrast, isolated 17-kD subunit itself has been reported to form a channel (Sun et al., 1987). In the present study, the permeability of proton in endosomes which were pretreated with OSW2 was rather higher (Fig. 7 *b*). The results strongly suggest that observed decrease in acidification could also be due to an increase in passive proton conductance. Although the suggestion that gating of the 17-kD proton pore is controlled by other subunits (Zhang et al., 1992) remains to be addressed, it is notable that the electrogenic nature of proton translocation requires co-transport of anions such as Cl^- or CO_3^-, or counter-transport of cations through channels. This property stresses that the movement of proton can be not only directly controlled by the gating of the pore for the ion but also indirectly by the mechanism for other ions (Forgac, 1989; Fuchs et al., 1989; see also Hille, 1992). Moreover, the primary structure of the 116-kD subunits appears to have a sufficient property of forming a channel (Perin et al., 1991). Including these points, we are currently addressing the effect of OSW2 on the ionic control in cells.

The specific nature of inhibition of the proton pumping by OSW2 contrasts to the effect of weak bases on the endosomal property. Weak bases diffuse nonspecifically into cells in their uncharged forms. In acidic compartments, they become protonated and are unable to diffuse out (Poole and Okuma, 1981). They, however, appear to have no property to close the existing ion-permeation mechanisms for other ions but can imbalance the fluxes. Thus, many kinds of amines induce vacuolization of late endosomes and lysosomes by the influx of water through translocation of proton (Okuma and Poole, 1981). This would also be the basis of the vesiculation of early endosomes by NH_4Cl (Fig. 10). These kinds of effects were not seen by the presence of OSW2, indicating that the antibody does not induce severe imbalancing of the water flux that leads to the structural disintegration. Moreover, in contrast to the inhibition of low pH in early compartments, pH in the later compartments was less influenced (Fig. 6). This property also contrasts to the effect of amines by which the magnitude of the elevation of pH is larger in more acidic compartments. By continuous incubation, OSW2 propagated in most of the compartments that are associated with the antigen, but at the same time, some in the perinuclear cluster remained free of its binding (Fig. 5). If assembly of the pump occurs during the transport with the endosomes, the effect on pH would be larger in early compartments. Along the further transport, the antibody reaching to the later compartments may be reduced by degradation. Even if it remained intact, as the pH in the close vicinity of the endosomal lumen can be lower than the average values, the antibody would likely less efficiently bind to the antigen on entering the already acidic late endosomal/lysosomal compartments. The result that cells incubated in the continuous presence of the antibody received no sizable effect on the cellular viability and growth suggests minor importance of early endosomal low pH for the cell survival.

Inhibition of the early endosomal compartments achieving low pH by OSW2 significantly reduced infections by all the enveloped viruses tested that possess fusion proteins activatable in low pH (influenza, SFV, VSV). The quenched R_{18}-fluorescence of internalized PR8 virus (Fig. 11) indicates a failure of uncoating by fusion. Reduced interference with the viral infection by the surface-bound antibody alone suggests that the binding to the internal reservoir of the compartments by fluid-phase endocytosis contributes in inhibiting acidification. The result that OSW2 did not compete with the adsorption of virus particles to cells rules out that the inhibition is based on events prior to uncoating. Experiments on the sequence of addition of the antibody further ruled out other mechanisms such as inhibition of transport of newly synthesized protein. Interference of infections by possible modification of endosome structure by cross-linking of the pro-

tein is unlikely the primary mechanism, since Fab fragment, albeit to a reduced extent, was also effective. The inhibition with 50–80% could be reasonably explained by the estimated average endosomal pH of 5.8 in antibody-treated cells (Fig. 6), which, although elevated from pH 5.2 in control cells, was around the threshold of the fusion dependence on pH (5.4–5.6 for PR8 virus, Sato et al., 1983; Yewdell et al., 1983; 6.0 for VSV, Matlin et al., 1982*b*; 6.0-6.2 for SFV, Kielian et al., 1986). The magnitude of interference was, however, significantly larger than a brief treatment with weak bases as it was more efficient in preventing viral fusion in endosomes (Fig. 11). These results provide another type of evidence for the early proposal stressing the primary importance of endosomal acidity in the viral infection. This point was, however, not fully proven by experiments employing amines or ionophores where side effects on cellular metabolism and on ER–Golgi were not fully ruled out (see Marsh and Helenius, 1989).

The present results indicate that the interference with the endosomal acidification by OSW2 provides a novel method for studying the endosomal proton pump. The luminal binding of OSW2 did not influence the peripheral to centripetal transfer (Figs. 4 and 5). Because the modification is specific to V-type pump and limited to the endosomal compartments, OSW2 looks more suitable for studying the role of the proton permeability in the endocytic processes than weak bases or ionophores. In yeast, mutational studies have indicated that the cells devoid of the pump activity become sensitive not only to high pH but also to the calcium concentration in the medium (Hirata et al., 1990; Noumi et al., 1991). Although binding of OSW2 is not cytotoxic, the role of the proton pump in the ionic control in conjunction with other ion-permeation mechanisms would deserve further study. As the endosome system can provide a sampling mechanism of the cellular environments (Anderson, 1991), application of OSW2-binding to V-type proton-pump would provide an insight to cell regulation mechanism using endosomes.

We would like to thank Ms. R. Keller and Ms. Y. Iida for excellent technical help, Dr. J. Yewdell for kindly providing monoclonal antibodies, Dr. Thomas Südhof for kindly providing the antiserum V759. We would like to show special thanks to Dr. Thomas Bächi at University of Zürich for encouragement and support of the initial part of this research.

Received for publication 12 May 1994 and in revised form 7 July 1994.

References

Adachi, I., K. Puopolo, N. Marquez-Sterling, H. Arai, and M. Forgac. 1990. Dissociation, cross-linking, and glycosylation of the coated vesicles proton pump. *J. Biol. Chem.* 265:967–973.

Anderson, R. G. W. 1991. Molecular motors that shape endocytic membrane. *In* Intracellular trafficking of proteins. C. J. Steer, and J. A. Hanover, editors. Cambridge University Press, New York. 13–46.

Arai, H., M. Berne, G. Terres, K. Puopolo, and M. Forgac. 1987. Subunit composition and ATP site labeling of the coated vesicles proton-translocating adenosinetriphosphatase. *Biochemistry.* 26:6632–6638.

Arai, H., G. Pink, and M. Forgac. 1988. Topography and subunit stoichiometry of the coated vesicle proton pump. *J. Biol. Chem.* 263: 8796–8802.

Bächi, T., M. Aguet, and C. Howe. 1973. Fusion of erythrocytes by Sendai virus studied by immuno-freeze-etching. *J. Virol.* 11:1004–1012.

Bächi, T., W. Gerhard, and J. Yewdell. 1985. Monoclonal antibodies detect different forms of influenza virus hemagglutinin during viral penetration and biosynthesis. *J. Virol.* 55:307–313.

Bowman, E. J., K. Tenny, and B. J. Bowman. 1988. Isolation of genes encoding the *Neurospora* vacuolar ATPase: analysis of *vma-1* encoding the 67-kDa subunit reveals homology to other ATPases. *J. Biol. Chem.* 263: 13994–14001.

Carlemalm, E., R. M. Garavito, and W. Villiger. 1982. Resin development for electron microscopy and an analysis of embedding at low temperatures. *J. Microscopy.* 126:123–143.

Dunn, K. W., and F. R. Maxfield. 1992. Delivery of ligand from sorting endosomes to late endosomes occurs by maturation of sorting endosomes. *J. Cell Biol.* 117:301–310.

Forgac, M. 1989. Structure and function of vacuolar class of ATP-driven proton pumps. *Physiol. Rev.* 69:765–796.

Fuchs, R., S. Schmid, and I. Mellman. 1989. A possible role for Na^+, K^+-ATPase in regulating ATP-dependent endosome acidification. *Proc. Natl. Acad. Sci. USA.* 86:539–543.

Galloway, C. J., G. E. Dean, M. Marsh, G. Rudnick, and I. Mellman. 1983. Acidification of macrophage and fibroblast endocytic vesicles *in vitro*. *Proc. Natl. Acad. Sci. USA.* 80:3334–3338.

Goldstein, J. L., M. S. Brown, R. G. W. Anderson, D. W. Russell, and W. J. Schneider. 1985. Receptor-mediated endocytosis: concepts emerging from the LDL receptor system. *Ann. Rev. Cell Biol.* 1:1–39.

Gruenberg, J., and K. E. Howell. 1989. Membrane traffic in endocytosis: insight from cell-free assays. *Ann. Rev. Cell Biol.* 5:453–481.

Harikumar, P., and J. P. Reeves. 1983. The lysosomal proton pump is electrogenic. *J. Biol. Chem.* 258:10403–10410.

Harlow, E., and D. Lane. 1988. Antibodies: A Laboratory Manual. Cold Spring Harbor Laboratory, Cold Spring Harbor, New York. 628–629.

Harvey, G. W., and N. Nelson, editors. 1992. V-ATPases *J. Exp. Biol.* 172:1–485.

Hille, B. 1992. Ionic channels of excitable membranes. 2nd edition. Sinauer Associates, Sunderland, MA.

Hirata, R., Y. Ohsumi, A. Nakano, H. Kawasaki, K. Suzuki, and Y. Anraku. 1990. Molecular structure of a gene, *VMA1*, encoding the catalytic subunit of H^+-translocating adenosine triphosphatase from vacuolar membranes of *Saccharomyces cerevisiae*. *J. Biol. Chem.* 265:6276– 6733.

Hirsch, S., A. Strauss, K. Masood, S. Lee, V. Sukhatme, and S. Gluck. 1988. Isolation and sequence of cDNA clone encoding the 31-kDa subunit of bovine kidney vacuolar H^+-ATPase. *Proc. Natl. Acad. Sci. USA.* 85: 3004–3008.

Hosoi, S., T. Nakamura, S. Higashi, T. Yamamuro, S. Toyama, K. Shinoyama, and H. Mikawa. 1982. Detection of human osteosarcoma-associated antigens by monoclonal antibodies. *Cancer Res.* 42:654–659.

Kane, P. M., C. T. Yamashiro, and T. H. Stevens. 1989. Biochemical characterization of the yeast vacuolar H^+-ATPase. *J. Biol. Chem.* 264:19236–19244.

Kane, P. M., M. C. Kuehn, I. Howald, and T. H. Stevens. 1992. Assembly and targeting of peripheral and integral membrane subunits of the yeast vacuolar H^+-ATPase. *J. Biol. Chem.* 267:447–454.

Kielian, M. C., M. Marsh, and A. Helenius. 1986. Kinetics of endosome acidification detected by mutant and wild type Semliki Forest virus. *EMBO (Eur. Mol. Biol. Organ.) J.* 5:3103–3109.

Laemmli, U. K. 1970. Cleavage of structural proteins during the assembly of the head of bacteriophage T4. *Nature (Lond.).* 227:680–685.

Mandel, M., Y. Moriyama, J. D. Hulmes, Y. C. Pan, H. Nelson, and N. Nelson. 1988. cDNA sequence encoding the 16-kDa proteolipid of chromaffin granules implies gene duplication in the evolution of H^+-ATPase. *Proc. Natl. Acad. Sci. USA.* 85:5521–5524.

Manolson, M. F., F. Ouellette, M. Filion, and R. J. Poole. 1988. cDNA sequence and homologies of the "57-kDa" nucleotide-binding subunit of the vacuolar ATPase from *Arabidopsis*. *J. Biol. Chem.* 263:17987– 17994.

Manolson, M. F., D. Proteau, R. Preston, A. Stenbit, B. T. Roberts, M. A. Hoyt, D. Preuss, J. Mulholland, D. Botstein, and E. W. Jones. 1992. The *VPH1* gene encodes a 95-kDa integral membrane polypeptide required for *in vivo* assembly and activity of the yeast vacuolar H^+-ATPase. *J. Biol. Chem.* 267:14294–14303.

Marsh, M., and A. Helenius. 1989. Virus entry into animal cells. *Adv. Virus Res.* 36:107–151.

Matlin, K. S., H. Reggio, A. Helenius, and K. Simons. 1982*a*. Infectious entry pathway of influenza virus in a canine kidney cell line. *J. Cell Biol.* 91: 601–613.

Matlin, K. S., H. Reggio, A. Helenius, and K. Simons. 1982*b*. Pathway of vesicular stomatitus virus entry leading to infection. *J. Mol. Biol.* 156: 609–631.

Matteoni, R., and T. E. Kreis. 1987. Translocation and clustering of endosomes and lysosomes depends on microtubules. *J. Cell Biol.* 105: 1253–1265.

Mellman, I., R. Fuchs, and A. Helenius. 1986. Acidification of the endocytic and exocytic pathways. *Ann. Rev. Biochem.* 55:663–700.

Moriyama, Y., and N. Nelson. 1989. Lysosomal H^+-translocating ATPase has a similar subunit structure to chromaffin granule H^+-ATPase complex. *Biochim. Biophys. Acta.* 980:241–247.

Noumi, T., C. Beltran, H. Nelson, and N. Nelson. 1991. Mutational analysis of yeast vacuolar H^+-ATPase. *Proc. Natl. Acad. Sci. USA.* 88: 1938–1942.

Nussbauman, O., and A. Loyter. 1987. Quantitative determination of virus-membrane fusion events: fusion of influenza virions with plasma membranes and membranes of endocytic vesicles in living cultured cells. *FEBS (Fed. Eur. Biochem. Soc.) Lett.* 221:61–67.

Okuma, K., and B. Poole. 1981. Cytoplasmic vacuolation of mouse peritoneal macrophages and uptake into lysosomes of weakly basic substances. *J. Cell Biol.* 90:656–664.

Parry, R. V., J. C. Turner, and P. A. Rea. 1989. High purity preparations of

higher plant vacuolar H^+-ATPase reveal additional subunits: revised subunit composition. *J. Biol. Chem.* 264:20025–20032.

Perin, M. S., V. A. Fried, D. K. Stone, and X.-S. Xie, and T. C. Südhof. 1991. Structure of the 116-kDa polypeptide of the clathrin-coated vesicle/synaptic vesicle proton pump. *J. Biol. Chem.* 266:3877–3881.

Poole, B., and S. Okuma. 1981. Effect of weak bases on the intralysosomal pH in mouse peritoneal macrophages. *J. Cell Biol.* 90:665–669.

Preston, R., R. F. Murphy, and E. W. Jones. 1987. Apparent endocytosis of fluorescein isothiocyanate-conjugated dextran by Saccharomyces cerevisiae reflects uptake of low molecular impurities, not dextran. *J. Cell Biol.* 105:1981–1987.

Puopolo, K., and M. Forgac. 1990. Functional reassembly of the coated vesicle proton pump. *J. Biol. Chem.* 265:14836–14841.

Puopolo, K., C. Kumamoto, I. Adachi, and M. Forgac. 1991. A single gene encodes the catalytic "A" subunit of the bovine vacuolar H^+-ATPase. *J. Biol. Chem.* 266:24564–24572.

Puopolo, K., C. Kumamoto, I. Adachi, R. Magner, and M. Forgac. 1992. Differential expression of the "B" subunit of the vacuolar H^+-ATPase in bovine tissues. *J. Biol. Chem.* 267:3696–3706.

Roberts, C. J., S. F. Nothwehr, and T. H. Stevens. 1992. Membrane protein sorting in the yeast secretory pathway: evidence that the vacuole may be the default compartment. *J. Cell Biol.* 119:69–83.

Sato, S. B., K. Kawasaki, and S. Ohnishi. 1983. Hemolytic activity of influenza virus hemagglutinin glycoproteins activated in mildly acidic environments. *Proc. Natl. Acad. Sci. USA.* 80:3153–3157.

Stegmann, T., H. W. M. Mordelt, J. Scholma, and J. Wilschut. 1987. Fusion of influenza virus in an intracellular acidic compartment measured by fluorescence dequenching. *Biochim. Biophys. Acta.* 904:165–170.

Stone, D. K., X.-S. Xie, and E. Racker. 1983. An ATP-driven proton pump in clathrin-coated vesicles. *J. Biol. Chem.* 258:4059–4062.

Stone, D. K., B. P. Crider, T. C. Südhof, and X.-S. Xie. 1989. Vacuolar Proton Pumps. *J. Bioenerg. Biomembr.* 21:605–620.

Südhof, T. C., V. A. Fried, D. N. Stone, P. A. Jhonston, and X.-S. Xie. 1989. Human endomembrane H^+-pump strongly resembles the ATP-synthetase of archaebacteria. *Proc. Natl. Acad. Sci. USA.* 86:6067–6071.

Sun, S. Z., X.-S. Xie, and D. K. Stone. 1987. Isolation and reconstitution of the dicyclohexylcarbodiimide-sensitive proton pore of the clathrin-coated vesicle proton translocating complex. *J. Biol. Chem.* 262: 14790–14794.

Towbin, H., T. Staehelin, and J. Gordon. 1979. Electrophoretic transfer of proteins from polyacrylamide gel to nitrocellulose sheet: procedure and some applications. *Proc. Natl. Acad. Sci. USA.* 76:4350–4354.

Wells, K. S., D. R. Sandison, J. Strickler, and W. W. Webb. 1990. Quantitative fluorescence imaging with laser scanning confocal microscopy. In Handbook of Biological Confocal Microscopy. J. B. Pawley, editor. Plenum Publishing, New York. 27–39.

Xie, X.-S., and D. K. Stone. 1988. Partial resolution and reconstitution of the subunits of the clathrin-coated vesicle proton ATPase responsible for Ca^{2+}-activated ATP hydrolysis. *J. Biol. Chem.* 263:9859–9867.

Yamashiro, D., S. R. Fluss, and F. R. Maxfield. 1983. Acidification of endocytic vesicles by an ATP-dependent proton pump. *J. Cell Biol.* 97:929–934.

Yewdell, J., W. Gerhard, and T. Bächi. 1983. Monoclonal anti-hemagglutinin antibodies detect irreversible antigenic alterations that coincide with the acid activation of influenza virus A/PR8/34-mediated fusion. *J. Virol.* 48: 239–248.

Yoshimori, T., A. Yamamoto, Y. Moriyama, M. Futai, and Y. Tashiro. 1991. Bafilomycin A_1, a specific inhibitor of vacuolar-type H^+-ATPase, inhibits acidification and protein degradation in lysosomes of cultured cells. *J. Biol. Chem.* 266:17707–17712.

Zhang, J., M. Myers, and M. Forgac. 1992. Characterization of the Vo domain of the coated vesicle (H^+)-ATPase. *J. Biol. Chem.* 267:9773–9778.

Zen, K., J. Biwersi, N. Periasamy, and A. S. Verkman. 1992. Second messengers regulate endosomal acidification in Swiss 3T3 fibroblasts. *J. Cell Biol.* 119:99–110.